

# Biochemical Characterization of a 22-kDa High Affinity Antiischemic Drug-Binding Polypeptide in the Endoplasmic Reticulum of Guinea Pig Liver: Potential Common Target for Antiischemic Drug Action

FABIAN F. MOEBIUS,<sup>1</sup> GREGORY G. BURROWS, JÖRG STRIESSNIG, and HARTMUT GLOSSMANN

*Institut für Biochemische Pharmakologie, Universität Innsbruck, A-6020 Innsbruck, Austria*

Received August 24, 1992; Accepted October 14, 1992

## SUMMARY

The phenylalkylamine emopamil prevents brain damage due to experimental cerebral ischemia. Stereoselective, high affinity, binding sites for (–)-[<sup>3</sup>H]emopamil in guinea pig brain cortex and liver membranes have been proposed to mediate its antiischemic effect. Using [*N*-methyl-<sup>3</sup>H]LU49888 as a photoaffinity probe we now provide evidence that the cation-sensitive emopamil binding site is localized on a 22-kDa polypeptide in guinea pig liver, kidney, lung, and adrenal gland. This 22-kDa polypeptide binds other antiischemic drugs with high affinity and is a nonglycosylated integral membrane protein of the endoplasmic reticulum. It can be solubilized with digitonin without changes in its drug-

binding properties. The solubilized binding activity has a sedimentation coefficient of  $12.0 \pm 0.4$  S and an apparent Stokes radius of  $6.0 \pm 0.1$  nm. From these data it is concluded that the 22-kDa polypeptide is associated in a larger oligomeric complex with a molecular mass of at least 84 kDa. [*N*-methyl-<sup>3</sup>H]LU49888 also specifically labels a second 27-kDa polypeptide in the endoplasmic reticulum, which can be distinguished from the 22-kDa polypeptide by its pharmacological and hydrodynamic properties. The photolabeled 22-kDa polypeptide was partially purified under denaturing conditions. This will allow the further structural analysis of this putative target for antiischemic drugs.

The phenylalkylamine (–)-emopamil is structurally related to the potent L-type Ca<sup>2+</sup> channel blockers (–)-verapamil and (–)-desmethoxyverapamil. It has, however, only weak Ca<sup>2+</sup> antagonistic properties but exhibits, in contrast to, for example, verapamil, pronounced antiischemic effects in a variety of experimental systems (1–5). The molecular mechanisms mediating these effects are unclear. Likewise, the biochemical events that are involved in ischemia-induced cell death in different tissues are not resolved and are a matter of controversy. Ischemia-induced formation of free radicals, lipid peroxidation, and activation of proteases and protein kinases are proposed (6, 7) to induce irreversible processes, eventually leading to rapid or delayed cell death. These processes are, at least in part, triggered by an elevation of the intracellular free

Ca<sup>2+</sup> ion concentration during or after ischemia (7). Prevention of cellular Ca<sup>2+</sup> overload in neuronal tissue by blocking glutamate-induced Ca<sup>2+</sup> influx with *N*-methyl-D-aspartate receptor antagonists provides one promising approach towards the reduction of ischemic tissue damage (8). Many chemically unrelated drugs, like emopamil, the antiarrhythmic amiodarone (9–11), the antidepressant opipramol (12), the antipsychotics trifluoperazine, chlorpromazine, and BMY-14802 (13, 14), and so called  $\sigma$  receptor drugs (15, 16) also exert antiischemic effects. It is at present unclear whether these drugs act via a common target or modulate completely different cellular functions leading to an increased tolerance against ischemic episodes. We recently characterized novel stereoselective, cation-sensitive, high affinity acceptor sites for the antiischemic phenylalkylamine (–)-[<sup>3</sup>H]emopamil, in different tissues, that are unrelated to phenylalkylamine binding domains on voltage-dependent L-type Ca<sup>2+</sup> channels (17). Subsequently we found that this novel binding site interacts with other antiischemic drugs with very high affinity. This suggested to us that the antiischemic effects

This work was supported by the Fonds zur Förderung der Wissenschaftlichen Forschung (S45-01 MED to H.G. and P9351 MED to J.S.) and by a grant from the Bundesministerium für Wissenschaft und Forschung.

<sup>1</sup> This paper is part of the doctoral thesis of F.F.M., to be presented to the Freie Universität Berlin.

**ABBREVIATIONS:** emopamil, 2-isopropyl-5-(methylphenethylamino)-2-phenylvaleronitrile hydrochloride;  $B_{max}$ , maximal density of binding sites; CHAPS, 3-[(3-cholamidopropyl)dimethylammonio]-1-propanesulfonate; CHAPSO, 3-[(3-cholamidopropyl)dimethylammonio]-2-hydroxy-1-propanesulfonate; [*N*-methyl-<sup>3</sup>H]LU49888, (–)-5-[(3-azidophenethyl)-[*N*-methyl-<sup>3</sup>H]methylamino]-2-(3,4,5-trimethoxyphenyl)-2-isopropylvaleronitrile; IC<sub>50</sub>, concentration causing half-maximal inhibition;  $k_{-1}$ , dissociation rate constant;  $k_{+1}$ , association rate constant; PAGE, polyacrylamide gel electrophoresis; PMSF, phenylmethylsulfonyl fluoride; SDS, sodium dodecyl sulfate; HEPES, 4-(2-hydroxyethyl)-1-piperazineethanesulfonic acid; 3-PPP, 3-(3-hydroxyphenyl)-*N*-(1-propyl)piperidine.

of drugs from different pharmacological classes might be mediated by a common target identified by (–)-[<sup>3</sup>H]emopamil. As an important step towards its identification we were prompted to identify the polypeptide carrying this drug acceptor site in different tissues and to study its biochemical, hydrodynamic, and pharmacological properties in guinea pig liver, where it occurs in high density (17). Our results presented below may pave the way to determining its primary structure. This will allow predictions about its physiological function and enable studies to clarify its possible pathophysiological role in ischemia-induced cell death. Sequence comparison with another polypeptide carrying a high affinity phenylalkylamine binding domain, the  $\alpha_1$  subunit of voltage-dependent L-type Ca<sup>2+</sup> channels (18), will help to reveal common structural features responsible for high affinity drug binding. In addition, evidence is presented suggesting that the 22-kDa polypeptide is pharmacologically related to a  $\sigma$  receptor subtype. Our studies should, therefore, also provide the basic tools for the further biochemical characterization of  $\sigma$  receptors.

## Experimental Procedures

**Materials.** (–)-[<sup>3</sup>H]Emopamil (≈67 Ci/mmol), [*N*-methyl-<sup>3</sup>H]LU49888 (≈80 Ci/mmol), the enantiomers of emopamil, and other unlabeled phenylalkylamines were kindly provided by Knoll A. G. (Ludwigshafen, Germany); (+)-3-PPP, (+)-SKF10,047, and 1,3-ditolylguanidine were a gift of Dr. Traber (Tropon, Cologne, Germany). Other chemicals were obtained from the following sources: opipramol, Ciba Geigy (Vienna, Austria); (±)-[<sup>125</sup>I]iodocyanopindolol, Amersham (Med-Pro, Vienna, Austria); digitonin and protease inhibitors, Sigma (Munich, Germany); Bradford protein reagent, electrophoresis reagents, and molecular weight markers, Bio-Rad; prestained molecular weight markers, BRL GIBCO (Dipro, Vienna).

**Binding assays.** Experiments with (–)-[<sup>3</sup>H]emopamil were performed as described (17). Briefly 1–2 nM emopamil was incubated with 0.02–0.03 mg/ml microsomal membranes in 10 mM Tris·HCl (pH 7.4), 0.1 mM PMSF (buffer A), at 25° for 60 min. Nonspecific binding was defined in the presence of 10  $\mu$ M (±)-emopamil. Drugs were diluted in dimethylsulfoxide and added directly to the incubation mixture. The final dimethyl sulfoxide concentration was ≤1% (v/v) (19), which did not affect (–)-[<sup>3</sup>H]emopamil binding. Binding to solubilized membranes was carried out in buffer A with a final concentration of 0.01–0.02% (w/v) digitonin. Bound and free ligand were separated by filtration over Whatman GF/C glass fiber filters after dilution of the incubation mixture with 4 ml of ice-cold 10% (w/v) polyethylene glycol 6000, 10 mM Tris·HCl (pH 7.4), 10 mM MgCl<sub>2</sub> (filtration buffer) (20). Solubilized protein was precipitated before filtration in the presence of 0.125 mg/ml bovine serum albumin and 0.125 mg/ml  $\gamma$ -globulin for 2 min on ice. Saturation analysis with (–)-[<sup>3</sup>H]emopamil was carried out by decreasing the specific activity of the radioligand with unlabeled (–)-emopamil. (±)-[<sup>125</sup>I]iodocyanopindolol binding assays were performed as described (21), using ligand concentrations of 5–7 pM and 0.1 nM propranolol to define nonspecific binding.

**Membrane preparation.** Crude microsomal membranes from different tissues were prepared from female guinea pigs as described (17). Briefly, tissues were trimmed free of connective tissue, minced with scissors, and homogenized on ice with a motor-driven glass-Teflon homogenizer in ice-cold 0.25 M sucrose, 10 mM Tris-HEPES (pH 7.4), with three complete strokes at 1800 rpm. The homogenate was centrifuged at 8000  $\times g$  in a SS-34 rotor and the resulting supernatant was collected by centrifugation at 40,000  $\times g$ . This microsomal pellet was washed twice with buffer A, resuspended at a concentration of 5–7 mg/ml membrane protein, frozen in liquid nitrogen, and stored at –80°. Protein was measured according to the method of Bradford (22), with bovine serum albumin as a standard.

**Photoaffinity labeling and SDS-PAGE.** [*N*-methyl-<sup>3</sup>H]LU49888 (7–16 nM) was incubated in the dark with 0.2 mg of microsomal membranes in buffer A for 60 min (final assay volume, 0.5 ml) at 22°. Samples of 0.025 ml were removed in triplicate to measure reversible binding before irradiation. The incubation mixture was then transferred to plastic Petri dishes (i.d., 35 mm) and irradiated for 55 sec with a Sylvania G15T8 UV lamp (10-cm distance). Nonspecific binding and photolabeling were defined with 1  $\mu$ M (+)-emopamil. Photolabeled membranes were collected by centrifugation and resuspended in 0.05 ml of buffer A containing 0.1% (w/v) SDS, 1 mM EDTA, 1  $\mu$ M pepstatin A, 0.1 mM benzamidine, and 1 mM iodoacetamide. Samples were denatured by addition of SDS-PAGE sample buffer (23) and incubated at 96° for 5 min. Solubilized membranes and fractions obtained from gel filtration and sucrose density gradients (0.03 mg of protein) were photolabeled with [*N*-methyl-<sup>3</sup>H]LU49888 in 0.5 ml of 0.1% (w/v) digitonin, 0.1 M KCl, 10 mM Tris·HCl (pH 7.4), 1 mM EDTA, 0.1 mM PMSF, 0.1 mM benzamidine, 1 mM iodoacetamide, 1  $\mu$ M pepstatin A (buffer B), as described above. After photolysis the protein was dialyzed overnight against 0.1% (w/v) SDS, 2.5 mM Tris·HCl (pH 6.8), lyophilized, and prepared for SDS-PAGE. SDS-PAGE was carried out on 12% polyacrylamide gels (24). Gels were calibrated using <sup>14</sup>C-labeled or prestained marker proteins. For fluorography Coomassie blue-stained gels were treated with Amplify (Amersham, Med-Pro, Vienna, Austria), dried, and exposed to Kodak X-Omat AR-5 or Chronex-4 films for the indicated times.

**Subcellular fractionation of guinea pig liver membranes.** Livers obtained from two male guinea pigs were immediately placed on ice, cleansed of connective tissue, minced with scissors, homogenized in ice-cold 0.25 M sucrose, 10 mM HEPES-KOH (pH 7.5), and fractionated as described for rat liver (25). The membrane fractions were flash frozen in liquid nitrogen and stored at –80°. Emopamil binding activity and the activity of the following marker proteins were determined in all fractions: glucose-6-phosphatase (endoplasmic reticulum) (26), alkaline phosphatase (apical plasma membrane) (27),  $\beta$ -adrenergic receptors ([<sup>125</sup>I]iodocyanopindolol binding; basolateral plasma membrane) (21), and succinate dehydrogenase (mitochondria) (28). The distribution of connexin 32 immunoreactivity was determined in Western blots as described (29), using sequence-directed antibodies raised against amino acid residues 98–124 of connexin 32 (30). Sera were kindly provided by Dr. D. A. Goodenough (Harvard Medical School, Department of Anatomy and Cellular Biology). Antibody binding was visualized using peroxidase-coupled goat anti-rabbit IgG (Sigma) and chemoluminescence detection (ECL, Amersham).

**Solubilization.** A stock solution of soluble 1.5% (w/v) digitonin was prepared as described (23). Membranes were resuspended at a protein to detergent ratio of 1:3.5 in 1% (w/v) digitonin, 0.1 M KCl, 10 mM Tris·HCl (pH 7.4), 0.1 mM PMSF, 1 mM EDTA, 0.1 mM benzamidine, 1 mM iodoacetamide, 1  $\mu$ M pepstatin A (buffer C), and were solubilized at 4° for 20 min. Insoluble material was removed by ultracentrifugation at 100,000  $\times g$  for 60 min. The supernatant was filtrated through Sartorius Minisart sterile filters (0.22  $\mu$ m). For some experiments peripheral membrane protein was removed by pretreating membranes with urea (2–5 M), 0.5 M KCl, 10 mM Tris·HCl (pH 7.4), with protease inhibitors, for 15 min at 22°. The extracted membranes were collected by ultracentrifugation and solubilized with digitonin as described above. Binding activity was also effectively solubilized in the zwitterionic detergents CHAPS and CHAPSO. However, the time-dependent formation of insoluble protein aggregates complicated their use for hydrodynamic studies and purification.

**Sucrose density gradient ultracentrifugation.** Two milliliters of supernatant and marker enzymes were layered onto 40-ml gradients of 5–30% (w/w) sucrose in buffer B and centrifuged for 165 min at 210,000  $\times g$  in a Beckman VTI-50 rotor. Twenty-four 1.6-ml fractions were collected from the bottom of the tube and assayed in duplicate for (–)-[<sup>3</sup>H]emopamil binding activity, protein concentration, sucrose density, and marker enzyme activity (31). All steps were carried out at 4°.

**Gel filtration chromatography.** One-half milliliter of solubilized material was applied to a TSK 3000 SW (600 × 7.5-mm) high performance liquid chromatography column (Pharmacia, Vienna, Austria) that had been equilibrated in buffer B and was eluted at 1.0 ml/min at 22°. Fractions (0.5 ml) were collected on ice and analyzed in duplicate for (–)-[<sup>3</sup>H]emopamil binding activity and total protein concentration. Marker enzymes (31) were run separately.

**Lectin chromatography.** Solubilized microsomal membranes (0.7 mg, 0.75 ml) in 0.33% (w/v) digitonin, 0.1 M KCl, 10 mM Tris·HCl (pH 7.4), 0.3 μM pepstatin A, 0.03 mM PMSF (buffer D), were incubated for 2.5 hr at 4° with 0.3 ml of Sepharose-coupled lectin (wheat germ agglutinin, *Ricinus communis* lectin, or concanavalin A) that had been equilibrated in 3 ml of buffer D. The Sepharose gel was removed by centrifugation and the supernatant was analyzed for (–)-[<sup>3</sup>H]emopamil binding and total protein concentration.

**Partial purification of the 22-kDa (–)-[<sup>3</sup>H]emopamil-binding protein by sucrose density gradient centrifugation of urea-extracted membranes and gel filtration in SDS.** Microsomal liver membranes (≈30 mg of protein) were collected by centrifugation and incubated for 15 min at 22° in 20 ml of 5 M urea, 0.5 M KCl, 10 mM Tris·HCl (pH 7.4), 1 mM EDTA, 0.1 mM PMSF, 0.1 mM benzamide, 1 mM iodoacetamide, 1 μM pepstatin A. After centrifugation (100,000 × *g*, 45 min, 4°) the pellets were solubilized in digitonin. Solubilized samples (4 ml) were separated on two 40-ml 5–30% (w/w) sucrose density gradients. For further purification by denaturing size-exclusion chromatography, fractions of sucrose density gradients containing (–)-[<sup>3</sup>H]emopamil binding activity were pooled and photolabeled with [*N*-methyl-<sup>3</sup>H]LU49888 (≈10 nM). The photolabeled sample was dialyzed overnight against 0.1% (w/v) SDS, 0.01 M sodium phosphate (pH 6.9), and concentrated with a Centrprep 10 (Amicon) ultrafiltration cell. Sodium phosphate buffer (1 M) was added to a final concentration of 0.1 M. After heating for 10 min at 96°, insoluble material was removed by centrifugation (40,000 × *g*, 30 min). Aliquots (≈0.5 mg of total protein) were applied to a TSK 3000 SW column that had been equilibrated in 0.1% (w/v) SDS, 0.1 M sodium phosphate (pH 6.9), 1 mM EDTA, 0.1 mM PMSF, 3 mM dithiothreitol, at 22° and were eluted (1 ml/min) in the same buffer. Fractions (1.0 ml) were collected, dialyzed against 0.1% (w/v) SDS, 2.5 mM Tris·HCl (pH 6.8), 0.05 mM PMSF, 0.1 mM EDTA, lyophilized, and separated by SDS-PAGE.

**Statistics.** Binding parameters ( $IC_{50}$ , slope factor,  $K_d$ , and  $B_{max}$ ) were calculated by nonlinear curve-fitting to the general dose-response equation (32) (displacement curves) or a rectangular hyperbola (saturation curves). Apparent molecular weights,  $s_{20,w}$  values, and the Stokes radius were calculated by linear regression from standard curves. Data are given as means ± standard deviations.

## Results

**Interaction of antiischemic drugs with (–)-[<sup>3</sup>H]emopamil binding sites.** We first examined the possibility that other antiischemic drugs display high affinity for the (–)-[<sup>3</sup>H]emopamil acceptor site. Indeed, this was the case (see Table 1). The most potent were the tricyclic antidepressant opipramol and the phenothiazines trifluoperazine and chlorpromazine. These drugs exert antiischemic effects in neuronal tissue (12, 13) as well as in the myocardium (phenothiazines) (33). The antipsychotic BMY-14802, which also has neuroprotective effects (14), was slightly less potent. We also tested drugs with high affinity for so-called  $\sigma$  binding sites that have been reported to exhibit antiischemic effects (15, 16). Table 1 shows that typical ligands for  $\sigma$  binding sites, such as 1,3-ditolyguanidine, (+)-3-PPP, and (+)-SKF10,047, showed markedly lower affinities. Therefore, the (–)-[<sup>3</sup>H]emopamil acceptor protein is not associated with  $\sigma$  receptors that have high affinity for these compounds. The nonspecific neuroprotective  $Ca^{2+}$  antagonist flunarizine (34) was a weak inhibitor. These data indicated that

TABLE 1

**High affinity interaction of different antiischemic drugs with (–)-[<sup>3</sup>H]emopamil acceptor sites in guinea pig liver microsomes, compared with  $\sigma$  ligands**

Guinea pig liver microsomal membranes (0.02–0.03 mg/ml) were incubated with (–)-[<sup>3</sup>H]emopamil (1.04–2.46 nM) for 60 min at 22° in the absence and presence of other drugs. Nonspecific binding was defined with 10 μM (±)-emopamil.  $IC_{50}$  values and slope factors were obtained by fitting the binding inhibition data to the general dose-response equation (32) by nonlinear curve-fitting. All drugs caused >90% inhibition of (–)-[<sup>3</sup>H]emopamil binding. Data are means ± standard deviations from two to six separate experiments.

Drugs	$IC_{50}$	$n_H$
nM		
Antiischemic drugs		
(–)-Emopamil	18.4 ± 2.6*	0.91 ± 0.1
Amiodarone	25.1 ± 3.0*	1.06 ± 0.13
Opipramol	12.8 ± 3.9	1.11 ± 0.13
Trifluoperazine	7.97 ± 1.6	1.07 ± 0.01
Chlorpromazine	14.2 ± 0.8	0.93 ± 0.05
BMY-14802	98.5 ± 11.9	0.89 ± 0.06
Flunarizine	>1000	
$\sigma$ Ligands		
Haloperidol	189 ± 26	0.89 ± 0.18
(±)-Pentacozine	498 ± 139	1.21 ± 0.03
(+)-3-PPP	2213 ± 22	0.89 ± 0.04
Cocaine	4320 ± 10	0.97 ± 0.07
1,3-Ditolyguanidine	6738 ± 2393	0.84 ± 0.16
(+)-SKF10,047	9299 ± 972	0.82 ± 0.06

\* Data were taken from Ref. 17.

a series of antiischemic drugs interact with the (–)-[<sup>3</sup>H]emopamil acceptor site with high affinity. To characterize biochemically a putative common target for antiischemic drug action, we identified the polypeptide carrying the high affinity (–)-[<sup>3</sup>H]emopamil acceptor site by photoaffinity labeling in different tissues and we partially purified it from guinea pig liver.

**Identification of the emopamil-binding polypeptide by photoaffinity labeling.** The highest densities of (–)-[<sup>3</sup>H]emopamil acceptor sites are found in guinea pig liver (≈35 pmol/mg of protein), kidney, adrenal, and lung and lower densities are found in brain and heart (17). In order to identify the polypeptide carrying this site, microsomal membranes of the tissues with the highest binding densities were photoaffinity labeled with [*N*-methyl-<sup>3</sup>H]LU49888. We previously used this photoreactive phenylazide to label the high affinity phenylalkylamine binding domain on the  $\alpha_1$  subunit of L-type  $Ca^{2+}$  channels in excitable tissues (35, 36). [*N*-methyl-<sup>3</sup>H]LU49888 is structurally related to emopamil. Racemic LU49888 binds to the (–)-[<sup>3</sup>H]emopamil acceptor site with a  $K_i$  of 16.3 ± 6.5 nM (17). Fig. 1 shows the fluorogram after separation of photolabeled guinea pig liver microsomes by SDS-PAGE. Only the labeling of two polypeptides, with apparent molecular masses of 27 ± 1 (10 experiments) and 22 ± 1 (10 experiments) kDa, was specific; it was completely prevented in the presence of 1 μM (+)-emopamil. Both polypeptides were also specifically labeled in microsomes of guinea pig kidney, adrenal gland, and lung, where they migrated with the same electrophoretic mobility as in liver membranes (data not shown). Their apparent molecular masses did not change upon reduction of disulfide bonds (Fig. 1). The specific photolabeling of the 22-kDa polypeptide was partially sensitive to the treatment with dithiothreitol (see Fig. 1, lanes 1) and was almost completely lost after boiling for 5 min in 2% (v/v)  $\beta$ -mercaptoethanol (data not shown), whereas the labeling of the 27-kDa band was unaffected. Sensitivity of the photoproducts of arylazide photoligands to nucleophilic attack in the  $\alpha_1$  subunits of L-type



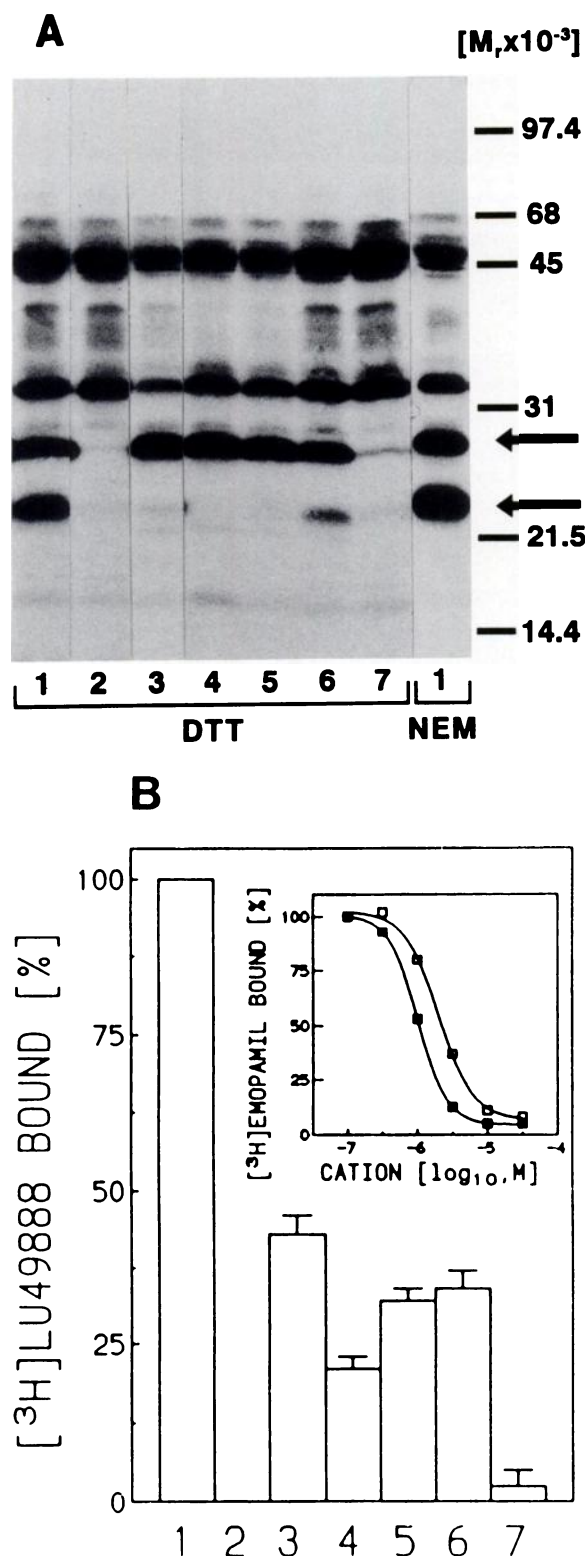


**Fig. 1.** Photoaffinity labeling of high affinity phenylalkylamine-binding polypeptides in guinea pig liver microsomal membranes with [*N*-methyl-<sup>3</sup>H]LU49888. **A**, Photolabeling. Guinea pig liver microsomal protein (0.2–0.4 mg/ml) was incubated in the dark with 15–17 nM [*N*-methyl-<sup>3</sup>H]LU49888 in the absence (lane 1) or presence of 1 μM (+)-emopamil (lane 2), 150 mM NaCl (lane 3), 0.05 mM ZnCl<sub>2</sub> (lane 4), 0.05 mM CdCl<sub>2</sub> (lane 5), 1 μM (+)-verapamil (lane 6), or 20 mM tetraethylammonium bromide (lane 7), irradiated with UV light, and separated by SDS-PAGE. A fluorogram (1-week exposure) of the dried gel is shown. Samples were separated under reducing (10 mM dithiothreitol present in the sample

Ca<sup>2+</sup> channels has been reported previously (37). This differential sensitivity of the covalent bonds formed between [*N*-methyl-<sup>3</sup>H]LU49888 and the two polypeptides suggested to us that their high affinity phenylalkylamine binding domains are structurally different.

To determine which polypeptide carries the cation-sensitive high affinity (–)-[<sup>3</sup>H]emopamil acceptor site identified in reversible binding studies (17), the pharmacological protection profile of photolabeling was investigated. Complete block of photolabeling by 1 μM (+)-emopamil suggests that both polypeptides bind (+)-emopamil with nanomolar affinity. Similar to reversible (–)-[<sup>3</sup>H]emopamil binding, photolabeling of both polypeptides was partially blocked by 1 μM (+)-verapamil (IC<sub>50</sub> for (–)-[<sup>3</sup>H]emopamil binding inhibition = 687 nM) (17) and was completely prevented by 20 mM tetraethylammonium (IC<sub>50</sub> = 1.8 mM) (17). In contrast, only [*N*-methyl-<sup>3</sup>H]LU49888 labeling of the 22-kDa polypeptide was modulated by mono- and divalent cations. It was completely blocked by 150 mM Na<sup>+</sup>, 0.05 mM Zn<sup>2+</sup>, or 0.05 mM Cd<sup>2+</sup> (Fig. 1A), whereas 150 mM K<sup>+</sup> was without effect (data not shown). Photolabeling of the high affinity phenylalkylamine binding site on the 27-kDa polypeptide was unaffected by these cations. Fig. 1B shows that about 30% of the reversible [*N*-methyl-<sup>3</sup>H]LU49888 binding before irradiation with UV light was insensitive to concentrations of cations that inhibit (–)-[<sup>3</sup>H]emopamil binding by >90% (Fig. 1B, inset). These differences in the cation sensitivity prove that the two photolabeled polypeptides carry related but distinct high affinity phenylalkylamine binding sites. The cation-sensitive acceptor site for (–)-[<sup>3</sup>H]emopamil and other antiischemic drugs is exclusively formed by the 22-kDa polypeptide. Under our assay conditions (–)-[<sup>3</sup>H]emopamil is a relatively selective ligand for the site on the 22-kDa polypeptide, whereas about 30% of reversible [*N*-methyl-<sup>3</sup>H]LU49888 binding is to the 27-kDa polypeptide (Fig. 1B).

**Preferential location of the 22-kDa polypeptide in the endoplasmic reticulum.** To further define the functional role of the (–)-[<sup>3</sup>H]emopamil acceptor site associated with the 22-kDa binding polypeptide, its subcellular localization in guinea pig liver membranes was determined. Membranes were fractionated by differential centrifugation as described for rat liver membranes (25). Enrichment of (–)-[<sup>3</sup>H]emopamil labeling in individual fractions was compared with the distribution of specific marker proteins. As shown in Table 2, binding activity was enriched 3–4-fold in the endoplasmic reticulum, together with glucose-6-phosphatase activity. No enrichment was found in mitochondria, nuclei, or the canalicular or basolateral plasma membrane. Golgi membrane fractions also contained (–)-[<sup>3</sup>H]emopamil binding, which can be explained by contamination

buffer) (DTT) or nonreducing (10 mM *N*-ethylmaleimide) (NEM) conditions. Arrows, specifically labeled polypeptides. **B**, Reversible binding of [*N*-methyl-<sup>3</sup>H]LU49888. Aliquots (0.025 ml) were removed in triplicates before irradiation to determine reversible [*N*-methyl-<sup>3</sup>H]LU49888 binding. Specific binding was calculated by subtracting binding in the presence of 1 μM (+)-emopamil (nonspecific binding) from total binding. Data from two experiments were normalized with respect to specific control binding and are given as means ± standard deviations. *Inset*, inhibition of (–)-[<sup>3</sup>H]emopamil (1.72 nM) binding to liver microsomal membranes (0.025 mg/ml membrane protein) by divalent cations. The following binding constants were calculated from two experiments: ZnCl<sub>2</sub> (■), IC<sub>50</sub> = 1.18 ± 0.18 μM, *n*<sub>H</sub> = 2.12 ± 0.09; CuCl<sub>2</sub> (□), IC<sub>50</sub> = 1.79 ± 0.02 μM, *n*<sub>H</sub> = 2.13 ± 0.14. The numbers under the bars correspond to the lane numbers in A.

TABLE 2

**Subcellular localization of the (–)-[<sup>3</sup>H]emopamil acceptor site associated with the 22-kDa polypeptide in guinea pig liver membranes**

Specific enzyme and binding activities were calculated from duplicate determinations at two or three different protein concentrations. Data from three preparations were pooled and are given as means  $\pm$  standard deviations. Ligand concentrations were 5–7 pM for [<sup>125</sup>I]iodocyanopindolol and 1.49–1.60 nM for (–)-[<sup>3</sup>H]emopamil. Specific activities in the homogenate were as follows (per mg of protein): (–)-[<sup>3</sup>H]emopamil binding,  $1.37 \pm 0.31$  pmol; glucose-6-phosphatase,  $1.66 \pm 0.4$   $\mu$ mol/hr; succinate dehydrogenase,  $76.31 \pm 8.79$  nmol/min; [<sup>125</sup>I]iodocyanopindolol binding,  $7.96 \pm 1.26$  fmol; alkaline phosphatase,  $2.37 \pm 0.4$   $\mu$ mol/hr. The total recovery of (–)-[<sup>3</sup>H]emopamil binding was 22.4%, with 20.4% being recovered in endoplasmic reticulum fractions. The following binding constants were measured for (–)-[<sup>3</sup>H]emopamil [ $K_d$  (nM)/ $B_{max}$  (pmol/mg) (two experiments)]: homogenate,  $6.12 \pm 1.97/7.08 \pm 0.81$ ; rough endoplasmic reticulum,  $6.70 \pm 2.03/19.94 \pm 1.70$ ; smooth endoplasmic reticulum,  $6.39 \pm 2.15/25.37 \pm 0.91$ ; Golgi apparatus,  $7.09 \pm 0.05/30.37 \pm 2.11$ .

Fraction	Specific activity					Recovery of (–)-[ <sup>3</sup> H]emopamil binding activity
	Emopamil binding	Glucose-6-phosphatase	Succinate dehydrogenase	$\beta$ -Adrenoceptor binding	Alkaline phosphatase	%
Homogenate	1.00	1.00	1.00	1.00	1.00	100
Heavy microsomes	$4.03 \pm 0.09$	$4.96 \pm 1.33$	$0.47 \pm 0.21$	$1.22 \pm 0.39$	$0.99 \pm 0.07$	$4.30 \pm 0.03$
Light microsomes	$3.66 \pm 0.10$	$4.26 \pm 0.69$	$0.44 \pm 0.22$	$1.57 \pm 0.60$	$1.03 \pm 0.22$	$6.68 \pm 2.24$
Rough endoplasmic reticulum	$3.32 \pm 0.22$	$5.13 \pm 1.55$	$0.38 \pm 0.13$	$1.14 \pm 0.47$	$1.12 \pm 0.29$	$4.46 \pm 0.52$
Smooth endoplasmic reticulum	$3.37 \pm 0.19$	$5.45 \pm 1.05$	$0.20 \pm 0.09$	$2.10 \pm 0.94$	$1.38 \pm 0.14$	$4.93 \pm 2.05$
Golgi apparatus	$3.68 \pm 0.54$	$3.68 \pm 1.47$	$0.65 \pm 0.17$	$2.38 \pm 0.87$	$1.65 \pm 0.62$	$0.24 \pm 0.16$
Light mitochondria	$0.17 \pm 0.08$	$0.31 \pm 0.13$	$3.72 \pm 0.11$	$0.09 \pm 0.03$	$0.59 \pm 0.18$	$1.14 \pm 0.54$
Heavy mitochondria	$0.54 \pm 0.22$	$0.59 \pm 0.37$	$3.27 \pm 0.30$	$3.72 \pm 2.22$	$2.06 \pm 0.23$	$0.38 \pm 0.00$
Nuclei	$0.72 \pm 0.14$	$0.40 \pm 0.11$	$1.53 \pm 0.40$	$0.51 \pm 0.33$	$0.62 \pm 0.20$	ND*
Cytosol	$0.19 \pm 0.04$	$0.29 \pm 0.05$	$0.17 \pm 0.10$	$0.06 \pm 0.01$	$0.61 \pm 0.09$	ND
Plasma membrane	$0.64 \pm 0.13$	$0.64 \pm 0.47$	$1.58 \pm 0.12$	$5.59 \pm 0.05$	$4.71 \pm 0.42$	$0.25 \pm 0.13$

\* ND, not determined.

with endoplasmic reticulum (i.e., by glucose-6-phosphatase activity). The dissociation constant of (–)-[<sup>3</sup>H]emopamil was unchanged in the microsomal fractions, compared with the homogenate (see legend to Table 2). The similarity of the molecular masses of the two photolabeled peptides to those of connexins 26 and 32 prompted us to study the distribution of connexin 32 immunoreactivity in the individual membrane fractions. As expected, the highest densities for connexin 32 were found in fractions enriched in plasma membranes, which contained low levels of (–)-[<sup>3</sup>H]emopamil binding activity. Identical results were obtained with purified rat liver plasma membranes (data not shown). Photoaffinity labeling of the isolated membrane fractions confirmed the co-purification of the 22-kDa polypeptide with (–)-[<sup>3</sup>H]emopamil binding activity in the endoplasmic reticulum membranes (Fig. 2; Table 2).

**Solubilization, hydrodynamic characterization, and partial purification.** To characterize further the biochemical and hydrodynamic properties of the 22-kDa polypeptide, guinea pig liver microsomes were solubilized under conditions preserving reversible (–)-[<sup>3</sup>H]emopamil and [*N*-methyl-<sup>3</sup>H]LU49888 binding activity. Treatment of membranes with 2 M urea/0.5 M KCl solubilized  $32 \pm 3\%$  (six experiments) of the membrane protein but only  $5 \pm 3\%$  (six experiments) of the membrane-associated (–)-[<sup>3</sup>H]emopamil binding activity. This indicates that the 22-kDa polypeptide is a hydrophobic, integral membrane protein. Binding activity could be efficiently solubilized using the nonionic detergent digitonin or the zwitterionic detergents CHAPS or CHAPSO at concentrations of 1% (w/v) and protein to detergent ratios of 1:3.5. Digitonin (1%, w/v) solubilized  $95 \pm 5\%$  (13 experiments) of the binding activity and  $81 \pm 12\%$  (13 experiments) of the membrane protein. The binding properties for (–)-[<sup>3</sup>H]emopamil did not change upon solubilization ( $k_{+1} = 0.022 \pm 0.001$  nM<sup>–1</sup> min<sup>–1</sup>,  $k_{-1} = 0.171 \pm 0.01$  min<sup>–1</sup>,  $K_d = 8.42 \pm 0.22$  nM,  $B_{max} = 29 \pm 1$  pmol/mg of protein; two experiments). The affinity and stereoselectivity for the drugs with high affinity for the (–)-[<sup>3</sup>H]emopamil acceptor site were not affected by solubilization (<10% change in apparent affinities; data not shown). Photoaffinity labeling

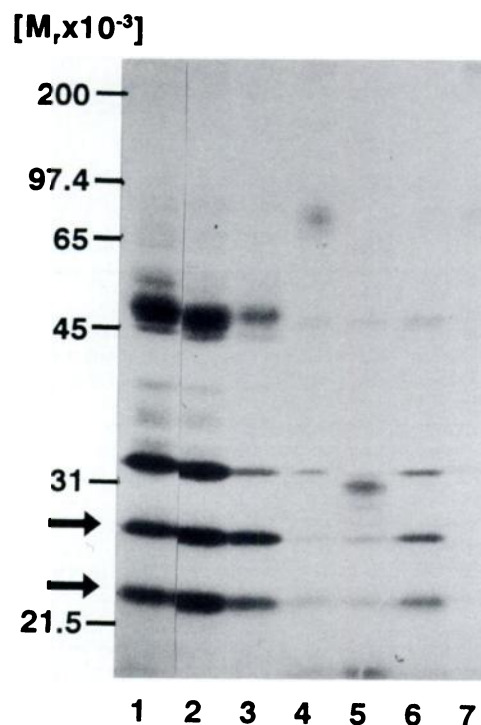


**Fig. 2.** [*N*-methyl-<sup>3</sup>H]LU49888 photolabeling of subcellular fractions. Protein (0.2 mg/ml) from the subcellular fractions (see Table 2) was photolabeled with 7.81 nM [*N*-methyl-<sup>3</sup>H]LU49888. Labeled membranes were collected by centrifugation, resuspended in sample buffer, and separated on 12% SDS-polyacrylamide gels. The fluorogram after 7 days of exposure is shown. Lane 1, homogenate; lane 2, light microsomes; lane 3, Golgi apparatus; lane 4, light mitochondria; lane 5, heavy mitochondria; lane 6, nuclei; lane 7, plasma membrane. The arrows indicate the migration of the 27-kDa and 22-kDa polypeptide.

of digitonin-solubilized membranes with [*N*-methyl-<sup>3</sup>H]LU49888 (Fig. 3, C and D, lanes SM) revealed that both specifically photolabeled polypeptides were extracted into the supernatant. To determine the molecular mass of the detergent-solubilized 22-kDa polypeptide, the sedimentation coefficient

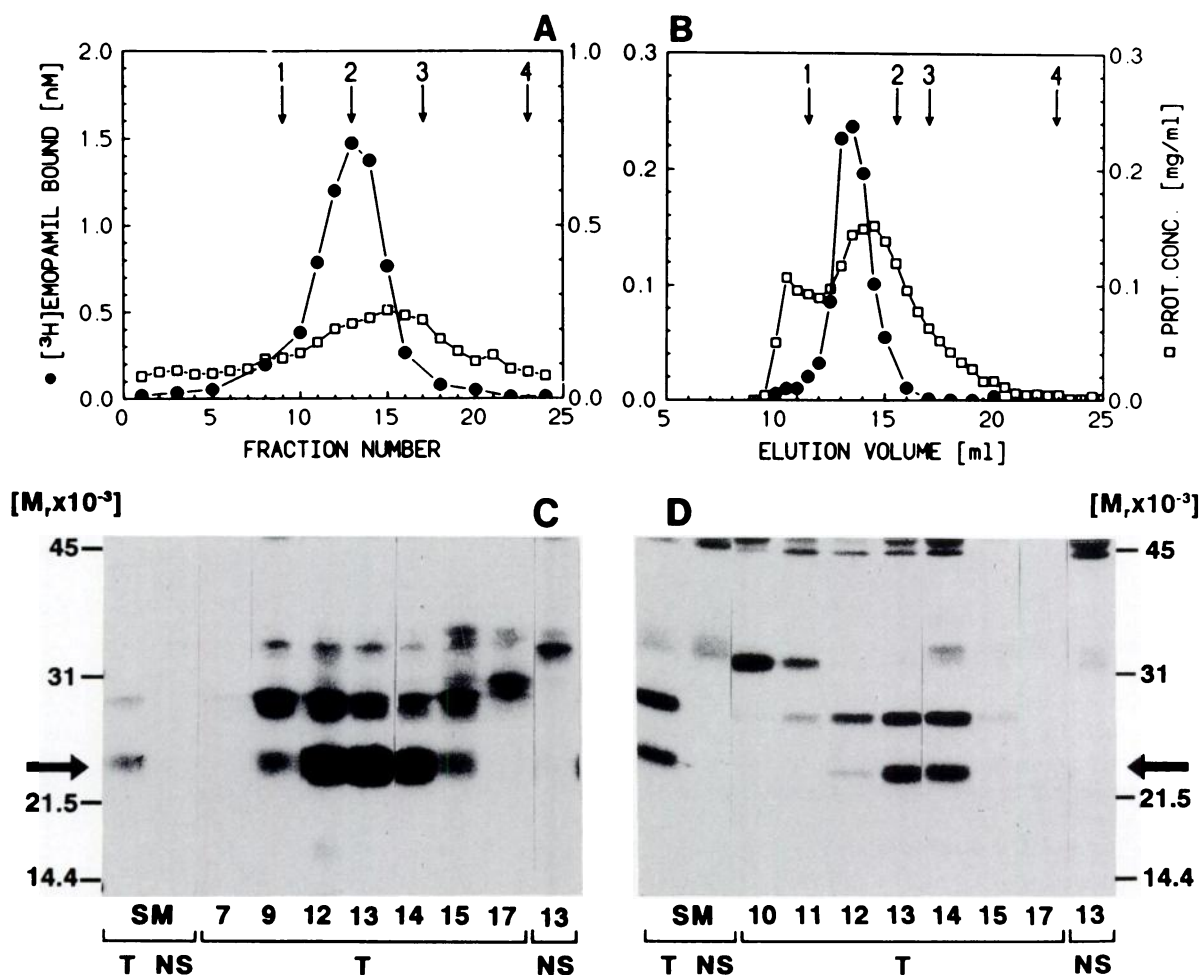


**Fig. 3.** Hydrodynamic characterization of the digitonin-solubilized 22-kDa polypeptide. A and B, Liver microsomes were solubilized with 1% (w/v) digitonin and 2 ml of solubilized membrane protein were separated on 40-ml 5–30% (w/w) sucrose density gradients (A). Fractions (1.6 ml) were collected and analyzed for reversible [ $^3\text{H}$ ]emopamil binding activity (ligand concentration, 1.48 nM) (●), total protein concentration (□), and marker enzyme activity. Alternatively, 0.5 ml of solubilized membranes was applied to a TSK 3000 SW gel filtration column (600  $\times$  7.5 mm) and eluted in buffer B at 1 ml/min (B). Fractions (0.5 ml) were collected and assayed as described above. A Stokes radius of 6.1 and a  $s_{20,w}$  value of 11.7 S were calculated by linear regression ( $r = 0.998$ ) of standard curves using the following standard proteins [ $s_{20,w}$  values (sec $^{-1}$ )/Stokes radii (nm)]: 1,  $\beta$ -galactosidase, 15.93/6.84; 2, catalase, 11.3/5.21; 3, lactate dehydrogenase, 7.3/4.75; 4, cytochrome c, 1.71/1.87. C and D, [ $N$ -methyl- $^3\text{H}$ ]LU49888 photolabeling of sucrose density gradient fractions (C) and fractions eluted from the size exclusion column (D). Protein (0.03 mg) from the fractions obtained in the experiments shown in A and B were photolabeled with [ $N$ -methyl- $^3\text{H}$ ]LU49888 (14–16 nm) in the presence (NS) and absence (T) of 1  $\mu\text{M}$  (+)-emopamil. After dialysis against 0.1% (w/v) SDS, 2.5 mM Tris-HCl (pH 6.8), samples were lyophilized and separated on 12% (w/v) SDS-polyacrylamide gels, and photolabeled polypeptides were visualized by fluorography (15-day exposure). Reversible (–)[ $^3\text{H}$ ]emopamil binding comigrated with the photolabeled 22-kDa polypeptide. SM, solubilized membranes. The arrow indicates the migration of the 22-kDa polypeptide.

( $s_{20,w}$ ) and the Stokes radius were determined by sucrose density gradient centrifugation (Fig. 3A) and size exclusion chromatography (Fig. 3B). (–)[ $^3\text{H}$ ]Emopamil binding activity migrated with an apparent  $s_{20,w}$  value of  $12.0 \pm 0.4$  S (five experiments) in sucrose gradients and eluted with an apparent Stokes radius of  $6.0 \pm 0.1$  nm (four experiments) from the gel filtration column. With a known partial specific volume of 0.715–0.829 ml/g for protein and bound digitonin (38, 39), a molecular mass between 280 and 515 kDa was calculated for the solubilized complex (for formula, see Ref. 31). The use of digitonin did not permit the direct determination of the amount of bound detergent. However, in hydrodynamic studies of other membrane proteins the contribution of digitonin to the total mass of the complex is known to range between 50 and 70% (40, 41). Therefore, the protein portion of the solubilized complex accounts for between 84 and 257 kDa, suggesting that the 22-kDa polypeptide is associated with itself or other nonphotolabeled subunits in an oligomeric complex.

To further prove that reversible (–)[ $^3\text{H}$ ]emopamil binding activity reflects only binding to the 22-kDa polypeptide, we analyzed the co-migration of the two phenylalkylamine binding polypeptides across the emopamil binding peak in sucrose density gradients (Fig. 3C) and eluates from gel filtration columns (Fig. 3D). Individual fractions were photoaffinity labeled with [ $N$ -methyl- $^3\text{H}$ ]LU49888 (Fig. 3, C and D) and analyzed by SDS-PAGE and fluorography. As expected, the intensity of the 22-kDa polypeptide labeling strictly correlated with the reversible (–)[ $^3\text{H}$ ]emopamil binding activity. In contrast, the 27-kDa polypeptide showed a slightly distinct separation profile in both separation procedures. This was evident as a change in the ratio of the intensities of the two photolabeled polypeptides across the binding peaks. In sucrose density gradients only a fraction of the 27-kDa band co-migrated with the binding activity (Fig. 3C) but this peptide was also enriched in fractions with higher sucrose density (see also Fig. 4A) corre-



sponding to the  $s_{20,w}$  value of  $\beta$ -galactosidase (15.9 S). Similarly, the 27-kDa polypeptide eluted with an apparent higher molecular weight from the gel filtration column (Fig. 3D). This separation suggests that the two phenylalkylamine-binding polypeptides are not associated with each other in the same oligomeric structure after digitonin solubilization. The 22-kDa polypeptide or putative associated subunits do not carry complex carbohydrates. Only 21%, 12%, and 8% of the solubilized binding activity and <10% of the total protein were adsorbed to the Sepharose-immobilized lectins concanavalin A, wheat germ lectin, and *R. communis* lectin, respectively. This precluded further purification by lectin affinity chromatography.

Further attempts to enrich reversible binding activity under nondenaturing conditions by hydrophobic interaction chromatography, cation or anion exchange chromatography, and chromatography on hydroxyapatite were complicated by the low recovery of reversible binding activity and photolabeled peptides from these matrices (data not shown). After urea treatment of microsomal membranes followed by separation of the digitonin-solubilized membrane protein on sucrose density gradients, the 22-kDa polypeptide was visible as a faint Coomassie-stained band strictly co-migrating with the specific photolabeling (Fig. 4, A and B). The photolabeled 22-kDa polypeptide could be further enriched by denaturing size-exclusion chromatography on a TSK 3000 SW column in phosphate buffer containing 0.1% SDS, which effectively separated it from the 27-kDa polypeptide (Fig. 4, C and D).

## Discussion

In this paper we report the identification of two high affinity phenylalkylamine-binding polypeptides with apparent molecular masses of 22 and 27 kDa in SDS gels and the partial purification of a photolabeled 22-kDa polypeptide that binds antiischemic drugs with high affinity. Both are specifically photoaffinity labeled by the arylazide phenylalkylamine [*N*-methyl- $^3\text{H}$ ]LU49888 and are localized in the endoplasmic reticulum.

Our data clearly rule out the possibility that these polypeptides are associated with  $\text{Ca}^{2+}$  channels. Voltage-dependent,  $\text{Ca}^{2+}$  antagonist-sensitive,  $\text{Ca}^{2+}$  channels are found in the plasma membrane of electrically excitable tissues but do not exist in the plasma membrane or the endoplasmic reticulum of liver cells. This is also evident from the absence of specific high affinity dihydropyridine [e.g., (+)- $^3\text{H}$ ]PN200-110] in this tissue (17). Moreover, high affinity [*N*-methyl- $^3\text{H}$ ]LU49888 photolabeling (Fig. 1) and [ $^3\text{H}$ ]emopamil binding to the 22-kDa polypeptide in liver membranes occur with a pharmacological profile clearly different from that of high affinity phenylalkylamine binding to the  $\alpha_1$  subunit of L-type  $\text{Ca}^{2+}$  channels (17, 35).

The differential sensitivity of the two [*N*-methyl- $^3\text{H}$ ]LU49888-photolabeled polypeptides to mono- and divalent cations allowed the unequivocal identification of the previously described cation-sensitive (–)- $^3\text{H}$ ]emopamil acceptor site (17) exclusively on the 22-kDa polypeptide. Its greater selectivity for (–)- $^3\text{H}$ ]emopamil and the lower chemical stability of its [*N*-methyl- $^3\text{H}$ ]LU49888 photolabeling provide additional evidence for subtle structural differences between the two labeled polypeptides. This finding also excludes the possibility that the two high affinity phenylalkylamine binding sites are identical but localized on different proteolytic breakdown products of a

larger precursor protein. Hydrodynamic studies revealed that the digitonin-solubilized polypeptides are associated in distinct oligomeric complexes (with themselves or other polypeptides) with apparent molecular masses between 84 and 257 kDa. The 22-kDa polypeptide is a nonglycosylated integral membrane protein localized in the endoplasmic reticulum. Its partial purification was achieved by sucrose density centrifugation of urea-extracted membranes followed by denaturing size-exclusion chromatography. This procedure should allow the isolation of larger amounts of this polypeptide for microsequencing to determine its primary structure.

Its molecular mass rules out its identity with metabolic enzymes such as the cytochrome P-450 family or flavin monooxygenases (molecular masses of >50 kDa) (42, 43). Members of a family of GTP-binding proteins recently identified in the endoplasmic reticulum membrane possess similar molecular masses (20–30 kDa) (44). Some of them are also associated in larger structures (about 100 kDa) (45) and are modulated by high concentrations of chlorpromazine (46). Because (–)- $^3\text{H}$ ]emopamil binding is insensitive to GTP and GTP analogues (17), a relationship between the 22-kDa polypeptide and these GTP-binding proteins is unlikely but cannot be completely excluded.

The 22-kDa polypeptide is not identical to previously described  $\sigma$  binding sites, which exist in the endoplasmic reticulum of different tissues (47, 48), inasmuch as several drugs such as 1,3-ditolylguanidine, (+)-3-PPP, and (+)-SKF10,047 were only weak inhibitors of (–)- $^3\text{H}$ ]emopamil binding. Instead, the pharmacological profile closely resembles that of a high affinity binding site for the antidepressant [ $^3\text{H}$ ]opipramol previously described in rat brain (49), which could define a novel subtype of  $\sigma$  binding sites. Therefore, the (–)- $^3\text{H}$ ]emopamil acceptor site appears to be closely related or perhaps identical to this site. Consequently, our work can also help to clarify the as yet unresolved functional and pharmacological role of  $\sigma$  binding sites (48). Recent studies also suggested that many drugs binding to  $\sigma$  sites exert neuroprotective effects (15, 16). Both the classical and the novel subtypes of  $\sigma$  binding sites (related to our 22-kDa polypeptide) could, therefore, represent potential targets for antiischemic drug action [see review by Ferris *et al.* (48)].

The localization of the 22-kDa polypeptide in the endoplasmic reticulum is interesting given the fact that morphological changes after transient ischemia are most pronounced in this organelle (50–52). Hippocampal CA1 neurons are especially sensitive to ischemia, and the ultrastructural changes preceding the observed “delayed neuronal death” involve marked proliferation of the endoplasmic reticulum and disaggregation of polyribosomes (50–52). Emopamil has been reported to prevent delayed neuronal death (3–5). It remains to be clarified whether the 22-kDa polypeptide plays a pathophysiological role in this process and whether modulation of its function by antiischemic drugs is responsible for their prevention of delayed neuronal death.

Knowledge of the structure of the 22-kDa polypeptide will also have implications for the understanding of the molecular organization of high affinity phenylalkylamine binding domains. The  $\text{Ca}^{2+}$  antagonist phenylalkylamine binding domain on the  $\alpha_1$  subunit of voltage-dependent L-type  $\text{Ca}^{2+}$  channels and the cation-sensitive (–)- $^3\text{H}$ ]emopamil acceptor site represent the only binding domains yet identified for phenylalkyl-

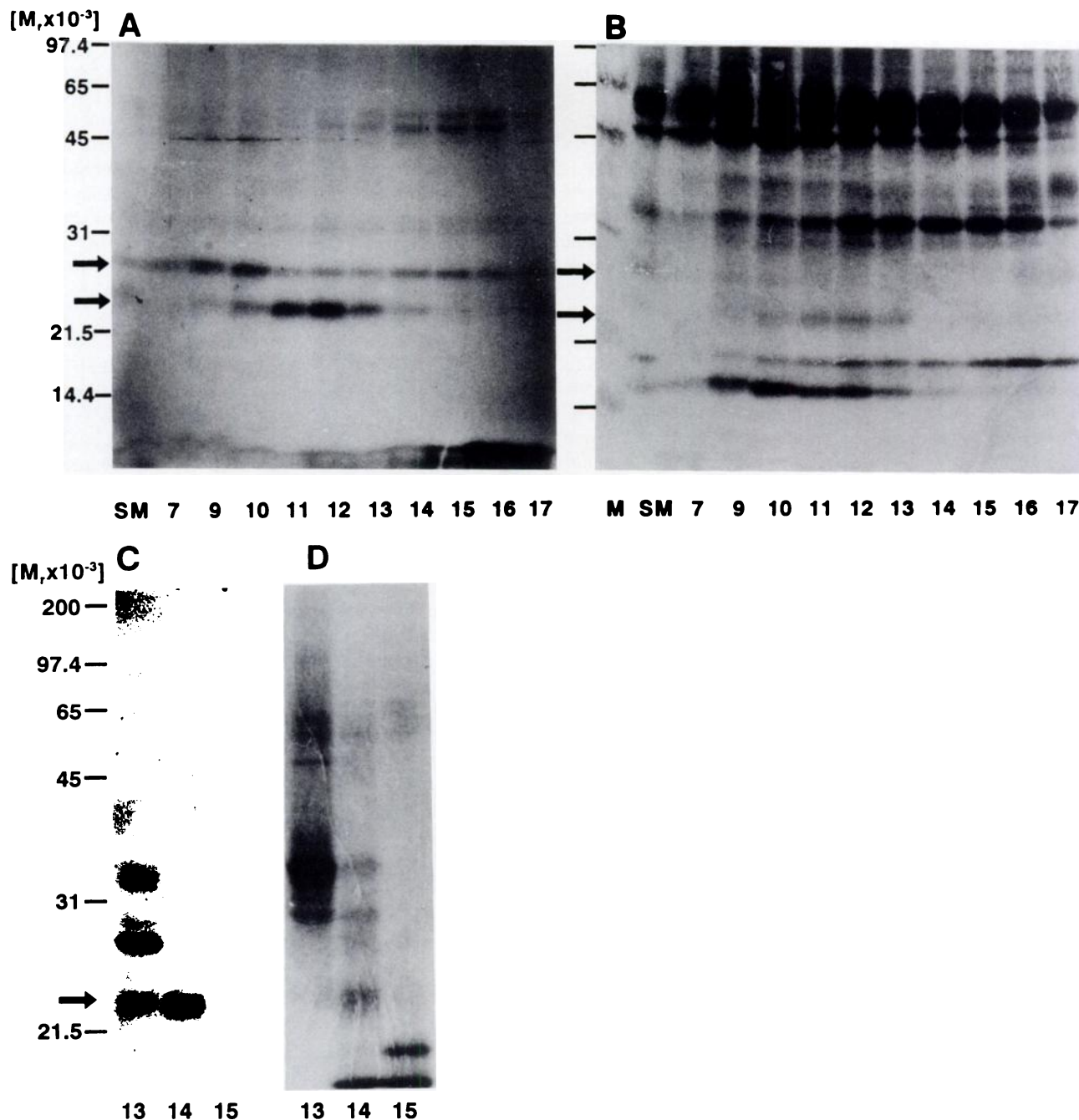


**Fig. 4.** Partial purification of the photolabeled 22-kDa polypeptide by sucrose density gradient centrifugation after urea extraction and denaturing SDS gel filtration. **A and B.** Sucrose gradient. Liver microsomal protein (29.6 mg) was photolabeled with 6.80 nM [*N*-methyl-<sup>3</sup>H]LU49888 in 30 ml of buffer A. Photolabeled microsomes were resuspended in 20 ml of 5 M urea, 0.5 M KCl, 0.01 M Tris·HCl (pH 7.4), containing protease inhibitors and were incubated for 15 min at 22°. After centrifugation for 60 min at 100,000 × *g*, 7.8 mg of protein and 75% of reversible [<sup>3</sup>H]emopamil binding were recovered in the pellet. The pellet was solubilized with digitonin as described in Experimental Procedures. Four milliliters of solubilized microsomes (4.7 mg of protein) and marker enzymes were layered on 5–30% (w/w) sucrose gradients and centrifuged for 165 min at 210,000 × *g*. The fractions obtained were analyzed for total radioactivity, protein concentration, marker enzyme activity, and reversible [<sup>3</sup>H]emopamil binding (at 2.05 nM ligand concentration, binding in fraction 12 was 8.5 pmol/mg). Samples containing 0.05 mg of protein were dialyzed overnight against 0.1% (w/v) SDS, 2.5 mM Tris·HCl, pH 6.8, lyophilized, resuspended in sample buffer, and analyzed on a 12% SDS-polyacrylamide gel. A fluorogram after 3 weeks of exposure (**A**) and the corresponding Coomassie stain (**B**) are shown. Fraction numbers are given; *M*, marker proteins; *SM*, solubilized microsomes. **Arrows**, two specifically labeled polypeptides. **C and D.** SDS gel filtration. Urea-treated membranes were solubilized and separated by sucrose density gradient centrifugation as in **A**. Fractions containing [<sup>3</sup>H]emopamil binding activity were pooled (1.8 mg of protein, 12 ml), photolabeled with [*N*-methyl-<sup>3</sup>H]LU49888 (6.8 nM), dialyzed against 0.1% (w/v) SDS, 0.01 M sodium phosphate, concentrated to 0.63 ml in a Centrprep 10 ultrafiltration cell, and denatured for 10 min at 96°. After centrifugation the sample was adjusted to 0.1 M sodium phosphate and a 0.15-ml aliquot (0.45 mg of protein) was applied to a TSK 3000 SW column and eluted in 0.1% (w/v) SDS, 0.1 M sodium phosphate, 0.1 mM PMSF, 1 mM EDTA, 3 mM dithiothreitol, at 1 ml/min (22°). Fractions (1 ml) were dialyzed against 0.1% (w/v) SDS, 2.5 mM Tris·HCl (pH 6.8), 0.05 mM PMSF, 0.1 mM EDTA, lyophilized, and separated on 12% polyacrylamide-SDS gels. A fluorogram of the dried gel is shown (14-day exposure). **D.** Coomassie stain of the gel shown in **C**. **Arrow**, migration of the 22-kDa polypeptide. The *numbers* indicate the elution volume (in milliliters) from the TSK-column.



lamines with a  $K_d$  in the low nanomolar range. Similar to L-type  $\text{Ca}^{2+}$  channels, this site can be efficiently labeled with [*N*-methyl- $^3\text{H}$ ]LU49888, which binds to  $\text{Ca}^{2+}$  channels ( $K_d = 2\text{--}3\text{ nM}$ ) and the 22-kDa polypeptide ( $K_i = 16\text{ nM}$  for racemic LU49888 and about 8 nM for the active enantiomer) (17) with comparable affinities. Therefore, the regions involved in the formation of the high affinity phenylalkylamine binding domain on the 22-kDa polypeptide can be determined using sequence-directed antibody mapping, as previously shown for L-type  $\text{Ca}^{2+}$  channels (18, 36). This will allow direct amino acid sequence comparison within these regions and could help to identify consensus structural features for high affinity phenylalkylamine binding.

The work presented here provides the basic tools for the further structural and functional characterization of a 22-kDa polypeptide that carries high affinity binding sites for a series of antiischemic drugs. The aim of future work will be to reveal the primary structure of this protein and its pathophysiological role in the development of irreversible ischemic damage. This can help the development of *in vitro* screening systems for the identification and optimization of antiischemic drugs, complementing the more time-consuming *in vivo* studies in animal models of focal and global ischemia.

#### Acknowledgments

The authors wish to thank Drs. Sidney and Becca Fleischer (Vanderbilt University, Nashville, TN) for providing samples of purified rat liver plasma membranes and advice on subcellular fractionation experiments. We are grateful to Dr. D. A. Goodenough for providing anticonnexin 32 antisera and helpful discussion. We thank the chemists and pharmacologists of Knoll A. G. (Ludwigshafen, Germany) for unlabeled and labeled phenylalkylamines and Dr. E. Schmid and M. Wimpfisser for expert technical assistance.

#### References

- Bielenberg, G. W., D. Sauer, J. Nuglisch, T. Beck, C. Roßberg, H. D. Mennel, and J. Kriegstein. Effects of emopamil on postischemic blood flow and neuronal damage in rat brain. *Naunyn-Schmiedeberg's Arch. Pharmacol.* **339**:230–235 (1989).
- Nakayama, H., M. D. Ginsberg, and W. D. Dietrich. S-Emopamil, a novel calcium channel blocker and serotonin  $\text{S}_2$  antagonist, markedly reduces infarct size following middle cerebral artery occlusion in the rat. *Neurology* **38**:1667–1673 (1988).
- Szabo, L., and H. P. Hofmann. (S)-Emopamil, a novel calcium and serotonin antagonist for the treatment of cerebrovascular disorders. 3, Effect on post-ischemic blood flow and metabolism, and ischemic neuronal death. *Drug Res.* **39**:314–319 (1989).
- Block, F., R. M. A. Jaspers, C. Heim, and K.-H. Sontag. S-Emopamil ameliorates ischemic brain damage in rats: histological and behavioural approaches. *Life Sci.* **47**:1511–1518 (1990).
- Lin, B., W. D. Dietrich, R. Busto, and M. D. Ginsberg. (S)-Emopamil protects against global ischemic brain injury in rats. *Stroke* **21**:1734–1739 (1990).
- Naylor, W. G. Basic mechanisms involved in the protection of the ischaemic myocardium: the role of calcium antagonists. *Drugs* **42** (Suppl. 2):21–27 (1991).
- Meldrum, B., and J. Garthwaite. Excitatory amino acid neurotoxicity and neurodegenerative disease. *Trends Pharmacol. Sci.* **11**:379–387 (1990).
- Choi, D. W., and S. M. Rothman. The role of glutamate neurotoxicity in hypoxic ischemic neuronal death. *Annu. Rev. Neurosci.* **13**:171–182 (1990).
- Karlson, J. A., R. W. Hopkins, J. M. Moran, and K. E. Karlson. Long-term amiodarone administration protects against global myocardial ischemia. *Ann. Thorac. Surg.* **50**:575–578 (1990).
- Vander Elst, L., J. F. Goudemant, J. Mouton, P. Chatelain, Y. Van Haverbeke, and R. N. Muller. Amiodarone pretreatment effects on ischemia isovolumic rat hearts: a P-31 nuclear magnetic resonance study of intracellular pH and high-energy phosphates contents evolutions. *J. Cardiovasc. Pharmacol.* **15**:377–385 (1990).
- Chatelain, P., M. Gremel, and R. Brotelle. Prevention by amiodarone of phospholipid depletion in isoproterenol-induced ischemia in rats. *Eur. J. Pharmacol.* **144**:83–90 (1987).
- Rao, T. S., J. A. Cler, S. J. Mick, D. M. Ragan, T. H. Lanthorn, P. C. Contreras, S. Iyengar, and P. L. Wood. Opipramol, a potent  $\sigma$  ligand, is an anti-ischemic agent: neurochemical evidence for an interaction with *N*-methyl-D-aspartate receptor complex *in vivo* by cerebellar cGMP measurements. *Neuropharmacology* **29**:1199–1204 (1990).
- Zivin, J. A., A. Kochhar, and T. Saitoh. Phenothiazines reduce ischemic damage to the central nervous system. *Brain Res.* **482**:189–193 (1989).
- Rao, T. S., J. A. Cler, S. J. Mick, S. Iyengar, and P. L. Wood. Inhibition of climbing and mossy fiber, and basket and stellate cell inputs to mouse cerebellar Purkinje cells by novel anti-ischemic agents, ifenprodil and BMV-14802. *Life Sci.* **47**:PL1–PL5 (1990).
- Pontecorvo, M. J., E. W. Karbon, S. Goode, D. B. Clissold, S. A. Borosky, R. J. Patch, and J. W. Ferkany. Possible cerebroprotective and *in vivo* NMDA antagonist activities of  $\sigma$  agents. *Brain Res. Bull.* **26**:461–465 (1991).
- Lobner, D., and P. Lipton.  $\sigma$ -ligands and non-competitive NMDA antagonists inhibit glutamate release during cerebral ischemia. *Neurosci. Lett.* **117**:169–174 (1990).
- Zech, C., R. Staudinger, J. Mühlbacher, and H. Glossmann. Novel sites for phenylalkylamines: characterization of a sodium-sensitive drug receptor with (–)-[ $^3\text{H}$ ]emopamil. *Eur. J. Pharmacol.* **208**:119–130 (1991).
- Catterall, W. A., and J. Striessnig. Receptor sites for  $\text{Ca}^{2+}$ -channel antagonists. *Trends Pharmacol. Sci.* **13**:256–262 (1992).
- Boer, R., A. Grassegger, C. Schudt, and H. Glossmann. (+)-Niguldipine binds with very high affinity to  $\text{Ca}^{2+}$  channels and to a subtype of  $\alpha_1$ -adrenoceptors. *Eur. J. Pharmacol.* **172**:131–145 (1989).
- Glossmann, H., and D. R. Ferry. Assay for calcium channels. *Methods Enzymol.* **109**:513–550 (1985).
- Kawai, Y., S. M. Graham, H. Yoshioka, and I. J. Anrinze.  $\beta$ -Adrenergic receptors in guinea-pig liver plasma membranes and thermal lability of [ $^3\text{H}$ ] dihydroalprenolol binding sites. *Biochem. Pharmacol.* **35**:4387–4393 (1986).
- Bradford, M. M. A rapid and sensitive method for the quantitation of microgram quantities of protein utilizing the principle of protein-dye binding. *Anal. Biochem.* **72**:248–254 (1976).
- Striessnig, J., K. Moosburger, A. Goll, D. R. Ferry, and H. Glossmann. Stereoselective photoaffinity labelling of the purified 1,4-dihydropyridine receptor of the voltage-dependent calcium channel. *Eur. J. Biochem.* **161**:603–609 (1986).
- Laemmli, U. K. Cleavage of structural proteins during the assembly of the head of bacteriophage T4. *Nature (Lond.)* **227**:680–685 (1970).
- Fleischer, S., and M. Kervina. Subcellular fractionation of rat liver. *Methods Enzymol.* **31**:6–41 (1974).
- Swanson, M. A. Glucose-6-phosphatase from liver. *Methods Enzymol.* **2**:541–543 (1961).
- Mircheff, A. K., and E. M. Wright. Analytical isolation of plasma membranes of intestinal epithelial cells: identification of Na,K-ATPase rich membranes and the distribution of enzyme activities. *J. Membr. Biol.* **28**:309–333 (1976).
- King, T. E. Preparations of succinate-cytochrome c reductase and the cytochrome b-c<sub>1</sub> particle, and reconstitution of succinate-cytochrome c reductase. *Methods Enzymol.* **10**:216–225 (1967).
- Grabner, M., K. Friedrich, H. G. Knaus, J. Striessnig, F. Scheffauer, R. Staudinger, W. J. Koch, A. Schwartz, and H. Glossmann. Calcium channels from *Cyprinus carpio* skeletal muscle. *Proc. Natl. Acad. Sci. USA* **88**:727–731 (1991).
- Goodenough, D. A., D. L. Paul, and L. Jesaitis. Topological distribution of two connexin 32 antigenic sites in intact and split rodent hepatocyte gap junctions. *J. Cell Biol.* **107**:1817–1824 (1988).
- Haga, T., K. Haga, and A. G. Gilman. Hydrodynamic properties of the  $\beta$ -adrenergic receptor and adenylate cyclase from wild type and variant S49 lymphoma cells. *J. Biol. Chem.* **252**:5776–5782 (1977).
- De Lean, A., P. J. Munson, and D. Rodbard. Simultaneous analysis of families of sigmoidal curves: application to bioassay, radioligand assay and physiological dose-response curves. *Am. J. Physiol.* **4**:E97–E102 (1978).
- Slezak, J., N. Tribulova, I. Gabauer, A. Iegelhoeffler, V. Holec, and J. Slezak. Diminution of "reperfusion" injury in reperfused ischemic myocardium by phenothiazines: a quantitative morphological study. *Gen. Physiol. Biophys.* **6**:491–512 (1987).
- Alps, B. J., C. Calder, W. K. Hass, and A. D. Wilson. Comparative protective effects of nicardipine, flunarizine, lidoflazine and nimodipine against ischemic injury in the hippocampus of the mongolian gerbil. *Br. J. Pharmacol.* **93**:877–883 (1988).
- Glossmann, H., and J. Striessnig. Molecular properties of calcium channels. *Rev. Physiol. Biochem. Pharmacol.* **114**:1–105 (1990).
- Striessnig, J., H. Glossmann, and W. A. Catterall. Identification of a phenylalkylamine binding region within the  $\alpha_1$  subunit of skeletal muscle  $\text{Ca}^{2+}$  channels. *Proc. Natl. Acad. Sci. USA* **87**:9108–9112 (1990).
- Striessnig, J., H. G. Knaus, and H. Glossmann. Photoaffinity-labelling of the calcium-channel-associated 1,4-dihydropyridine and phenylalkylamine receptor in guinea-pig hippocampus. *Biochem. J.* **253**:39–47 (1988).
- Baron, B., M. Gavish, and M. Sokolovsky. Heterogeneity of solubilized muscarinic cholinergic receptors: binding and hydrodynamic properties. *Arch. Biochem. Biophys.* **240**:281–296 (1985).
- Allen, R. A., A. J. Jesaitis, L. A. Sklar, C. G. Cochrane, and R. G. Painter. Physicochemical properties of the *N*-formyl peptide receptor on human neutrophils. *J. Biol. Chem.* **261**:1854–1857 (1986).
- Berrie, C. P., N. J. M. Birdsall, K. Haga, T. Haga, and E. C. Hulme. Hydrodynamic properties of muscarinic acetylcholine receptors solubilized from rat forebrain. *Br. J. Pharmacol.* **82**:839–851 (1984).
- Horne, W. A., G. A. Weiland, and R. E. Oswald. Solubilization and hydrodynamic characterization of the dihydropyridine receptor from rat ventricular muscle. *J. Biol. Chem.* **261**:3588–3594 (1986).
- Nebert, D. W., D. R. Nelson, M. J. Coon, R. W. Estabrook, R. Feyereisen, Y.

- Fujii-Kuriyama, F. J. Gonzales, F. P. Guengerich, I. C. Gunsalus, E. F. Johnson, J. C. Loper, R. Sato, M. R. Waterman, and D. J. Waxman. The P450 superfamily: update on new sequences, gene mapping, and recommended nomenclature. *DNA* **10**:1-14 (1991).
43. Ziegler, D. M. Flavin-containing monooxygenases: enzymes adapted for multisubstrate specificity. *Trends Pharmacol. Sci.* **11**:321-324 (1990).
  44. Takai, Y., K. Kaibuchi, A. Kikuchi, and M. Kawata. Small GTP-binding proteins. *Int. Rev. Cytol.* **133**:187-230 (1992).
  45. Shirataki, H., K. Kaibuchi, T. Yamaguchi, K. Wada, H. Horiuchi, and Y. Takai. A possible target protein for *smg-25A/rab3A* small GTP-binding protein. *J. Biol. Chem.* **267**:10946-10949 (1992).
  46. Kim, Y. S., A. Kikuchi, and Y. Takai. Effect of chlorpromazine on the *smg* GDS action. *Biochem. Biophys. Res. Commun.* **182**:1446-1453 (1992).
  47. Walker, J. M., W. D. Bowen, F. O. Walker, R. R. Matsumoto, B. De Costa, and K. C. Rice. *Sigma* receptors: biology and function. *Pharmacol. Rev.* **42**:355-402 (1990).
  48. Ferris, C. D., D. J. Hirsch, B. P. Brooks, and S. H. Snyder. *Sigma* receptors: from molecule to man. *J. Neurochem.* **57**:729-737 (1991).
  49. Ferris, C. D., D. J. Hirsch, B. P. Brooks, A. M. Snowman, and S. H. Snyder. [<sup>3</sup>H]Opipramol labels a novel binding site and *sigma*-receptor in rat brain membranes. *Mol. Pharmacol.* **39**:199-204 (1991).
  50. Kirino, T., and K. Sano. Fine structural nature of delayed neuronal death following ischemia in the gerbil hippocampus. *Acta Neuropathol. (Berl.)* **62**:209-218 (1984).
  51. Yamamoto, K., T. Hayakawa, H. Mogami, F. Akai, and T. Yanagihara. Ultrastructural investigation of the CA1 region of the hippocampus after transient cerebral ischemia in gerbils. *Acta Neuropathol. (Berl.)* **80**:487-492 (1990).
  52. Deshpande, J., K. Bergstedt, T. Linden, H. Kalimo, and T. Wieloch. Ultrastructural changes in the hippocampal CA1 region following transient cerebral ischemia: evidence against programmed cell death. *Exp. Brain Res.* **88**:91-105 (1992).

---

Send reprint requests to: Dr. Jörg Striessnig, Institut für Biochemische Pharmakologie, Peter Mayrstrasse 1, A-6020 Innsbruck, Austria.

---